Review of satellite derived irrigated cropping areas for the unregulated properties in the Namoi valley

DPE – WATER

SEPT 2023

alluvium

Alluvium recognises and acknowledges the unique relationship and deep connection to Country shared by Aboriginal and Torres Strait Islander people, as First Peoples and Traditional Owners of Australia. We pay our respects to their Cultures, Country and Elders past and present.

Artwork by Melissa Barton. This piece was commissioned by Alluvium and tells our story of caring for Country, through different forms of waterbodies, from creeklines to coastlines. The artwork depicts people linked by journey lines, sharing stories, understanding and learning to care for Country and the waterways within.

This report has been prepared by Alluvium Consulting Australia Pty Ltd for Department of Planning & Environment (DPE) under the contract titled 'Identification of satellite derived irrigated cropping areas in the Namoi valley to support the DPE Floodplain Harvesting Team'.

Authors:	Chris Sherwin
Review:	Rakesh Joshi, Ha Nguyen, Petter Nyman, Paul Richards, and Neal Albert
Approved:	Neal Albert
Version:	3.0 - Final
Date issued:	16/09/2023
Issued to:	Department of Planning & Environment (DPE)
Citation:	Alluvium, 2023, 'Review of satellite derived irrigated cropping areas for the unregulated properties in the Namoi valley', report prepared by Alluvium Consulting Australia for the DPE, NSW.
Cover image:	abstract river image, Shutterstock

alluvium

Contents

Figures

Tables

Summary

The Department of Planning and Environment (DPE) is using remote sensing to determine irrigated crop areas in the Namoi valley (NSW), and the outputs will inform water entitlements for unregulated floodplain harvesting based on historical use. Alluvium was engaged to review work undertaken to date and support DPE in this process. There were three objectives for this assessment:

1. **Verify the workflow** to ensure appropriate processing of Landsat imagery and classification of cropped areas into irrigated and non-irrigated land. This involved examining all geoprocessing steps in the assessment and verifying that these steps led to: 1) accurate data for the Normalised Difference Vegetation Index (NDVI) and 2) correct land use classification based on empirically derived NDVI thresholds.

2. **Apply an enhancing approach to see if the performance can be improved** by refining the method for handling Landsat imagery, filtering for artefacts, and objectively setting NDVI thresholds that discriminate between irrigated and non-irrigated areas. This involved automating the process by building a scripted workflow that is efficient and flexible.

3. **Apply the method to a case study area** located outside of the current reported regions of interest, to help determine levels of certainty in final outputs.

The key findings and outcomes of this assessment were:

- The Normalised Difference Vegetation Index (NDVI), which has been used by DPE for assessment of irrigated crop areas, is a well-established remote sensing method to measure canopy greenness (based on its sensitivity to plant canopy chlorophyll content) and a suitable metric to identify irrigated summer season crop areas in the Namoi valley.
- The summer growing season (December to March) is ideal to capture crop-specific optical signals (or signatures), which are critical in discerning irrigated crops from other land uses. The assumption was that irrigated crops are associated with unstressed signals compared to non-irrigated crops, given that irrigated crops do not experience the same water and/or heat stress. At the same time, both irrigated and non-irrigated crops are expected to have a dynamic signal compared to persistent vegetation like forests or plantations.
- An automated script for identifying irrigated crop areas was developed. This builds an objective and systemised manner into the assessment, with two key benefits assisting the current manual image processing method:
    - NDVI thresholds at the property level are defined through an iterative and non-subjective process.
    - The impacts of rainfall, clouds, and heat and water stress, as well as satellite scaling, are each considered and documented in this report.
- DPE's existing method is based on manual and subjective setting of NDVI thresholds, which could be a source of error at the property level because it relies heavily on human perception and experience level of analyst. Whilst a key outcome from this project is an automated objective approach, in defining what areas are irrigated crop, the end conclusional accuracy will be ensured by a trained analyst via a manual subjective method (focussing on crop tone, texture, rainfall impacts and possible misclassification).

1 Introduction

Alluvium was engaged by the Department of Planning and Environment (DPE) to review and confirm the workflow methods of using a remote sensing approach to determine irrigated crop areas in the Namoi valley was sound and based on scientific rigour. Mapping the irrigated crop areas is intended to inform the setting of water entitlements for floodplain harvesting based on historical use. There are 53 properties in the Namoi Valley that have been determined as eligible for an unregulated floodplain harvesting (FPH) entitlement, 31 of which relate to groundwater and 22 to an unregulated water source.

The objectives of the assessment undertaken by Alluvium were to:

- Verify the workflow undertaken by DPE to ensure appropriate processing of Landsat imagery and classification of cropped areas into irrigated and non-irrigated land. This involved examining all geoprocessing steps in the assessment and verifying that these steps led to both accurate data on Normalised Difference Vegetation Index (NDVI) and correct land use classification based on empirically derived NDVI thresholds. The period of interest for this analysis is 1993/94 to 1999/2000.

  This objective is addressed in:
  Section 3: DPE methods documentation and review outcomes
  Section 4: Detailed manual DPE method (step by step)
  Section 11: References

- Apply an enhancing approach to see if the performance can be improved by refining the method used by DPE to handle Landsat imagery, filter for artefacts, and objectively set NDVI thresholds that discriminate between irrigated and non-irrigated areas. This involved providing an automated (scripted) workflow that can be repeated across any set of landowner properties (where each property is referred to as a Region of Interest orROI). The scripted method forms a sensitivity analysis that considers the impact of environmental factors (e.g., rainfall, cloud effect and heat waves) and satellite scaling factors on the mapped irrigated crop areas at the property scale.

  This objective is addressed in:
  Section 5: Scripted method enhancements
  Section 6: Enhanced scripted workflow summary of the 3 modules
  Section 7: Comparative output assessment (DPE vs Alluvium methods)
  Section 8: Summary of output (enhanced scripted workflow)

- Apply the method to a case study area located outside of the current reported regions of interest, to help determine levels of certainty in final outputs.

  This objective is addressed in:
  Section 9: Enhanced scripted workflow validation (using Evapotranspiration, ET)
  Section 10: Conclusions.

2 DPE methods documentation and review outcomes

2.1 Study area

The study area is located in an agricultural area of the Namoi River catchment, which is part of the Murray Darling Basin (MDB) and the food bowl of Australia (House of Representatives Standing Committee on Regional Australia 2011). The Namoi valley comprises two distinct geographical zones – the Northern and Southern regions (Donaldson & Heath, 1997). These areas are also referred to as the Lower Namoi and Upper Namoi, as shown in Figure 1 and Figure 2 respectively.

There are several relevant policies and instruments which regulate the use of water resources in this area, including but not limited to:

- Water Sharing Plan for the Namoi and Peel Unregulated Rivers Water Sources (2012)
- Water Sharing Plan for the Namoi Alluvial Groundwater Sources Order (2020)
- Water Management (General) Amendment (Floodplain Harvesting Access Licences) Regulation 2022
- NSW Floodplain Harvesting Policy (September 2018)

The two regions are characterised by two main Koppen-Gieger climate types: Humid subtropical (Cfa) to the east and hot steppe (BSh) to the west (Beck et al., 2018). Mean annual rainfall in the Namoi valley varies between 449 to 1135 mm, with most rainfall occurring in summer and the northern regions being wetter than the south (Bureau of Meteorology, 2021). The topography is dominated by highlands in the south and east and a floodplain in the west, with the lowest elevation occurring near Walgett in the far northwest (Welsh et al., 2014). Complex tributary systems and flat topography makes it conducive to surface or furrow irrigation (Hope & Bennett, 2002). The most common soil type in the region, Grey and Brown Vertosols, is characterised by a high clay content and water holding capacity (34–42% v/v) (Dalgliesh et al., 2012; Isbell, 2016). Cotton is the dominant irrigated crop, covering over 60% of the irrigated area (Green et al., 2011).

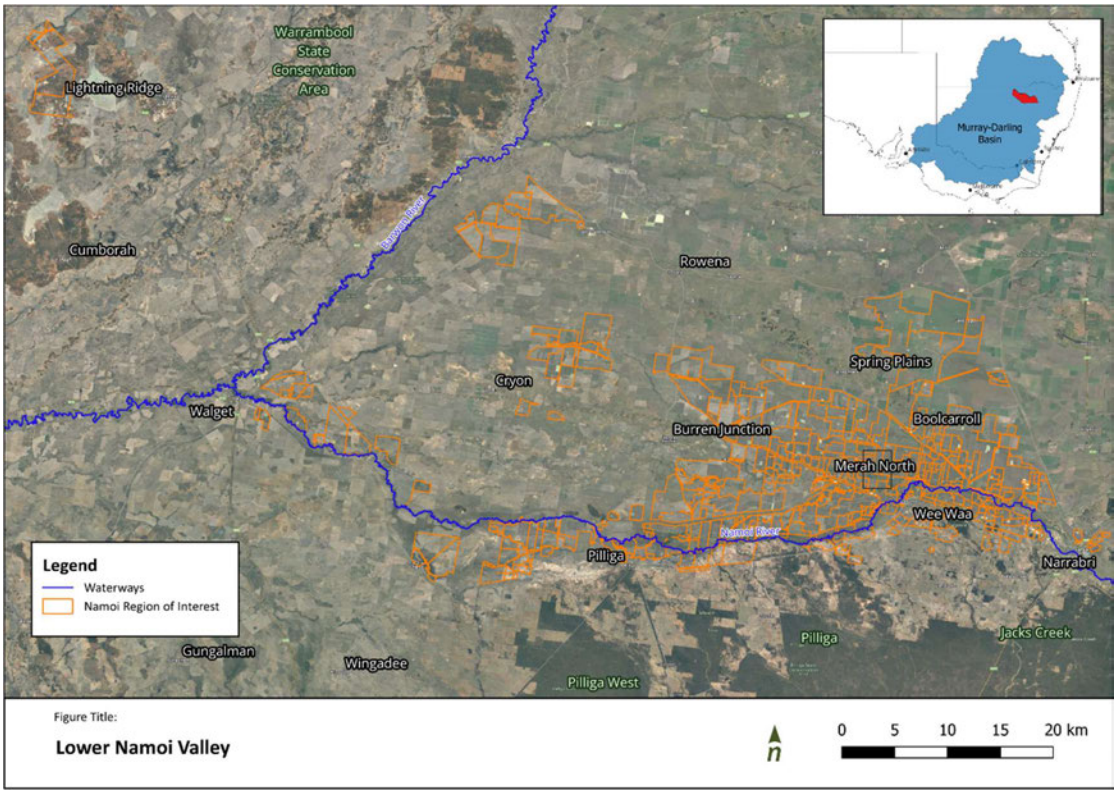

Figure 1: *Area of interest in the Lower Namoi, NSW.*

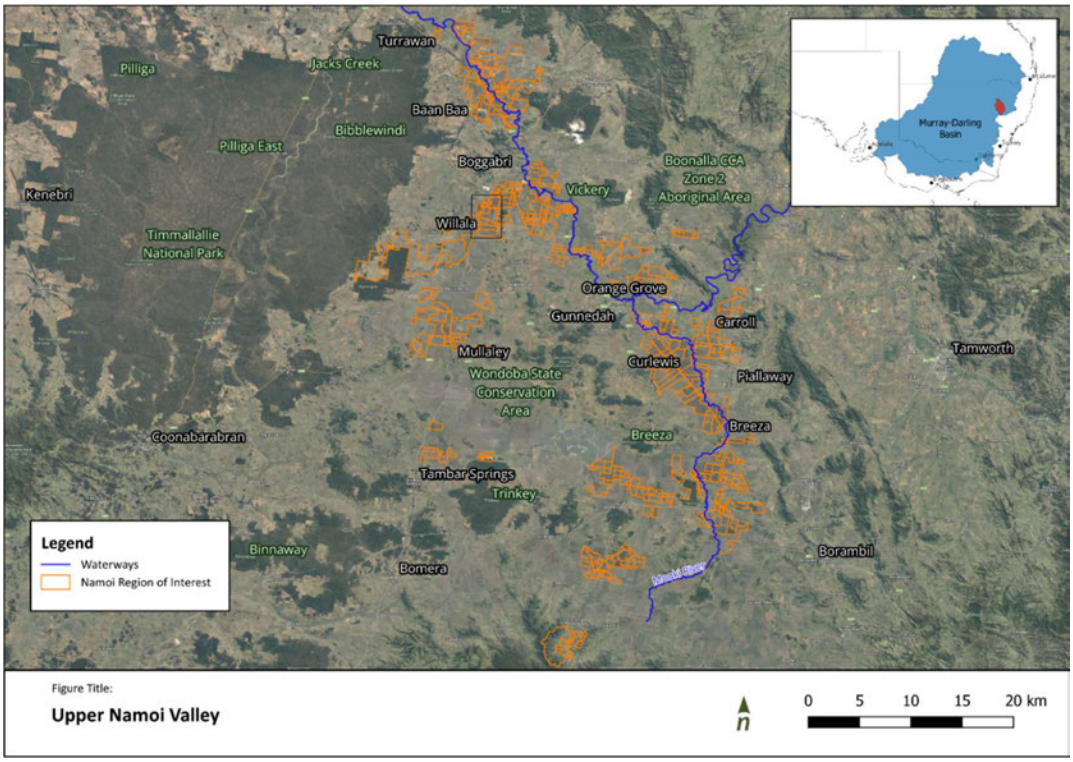

Figure 2: *Area of interest in the Upper Namoi, NSW.*

2.2 Method overview

A high-level representation of our method is shown in Figure 3, where red boxes are sections identified as sources of significant error and with the possibility of revision.

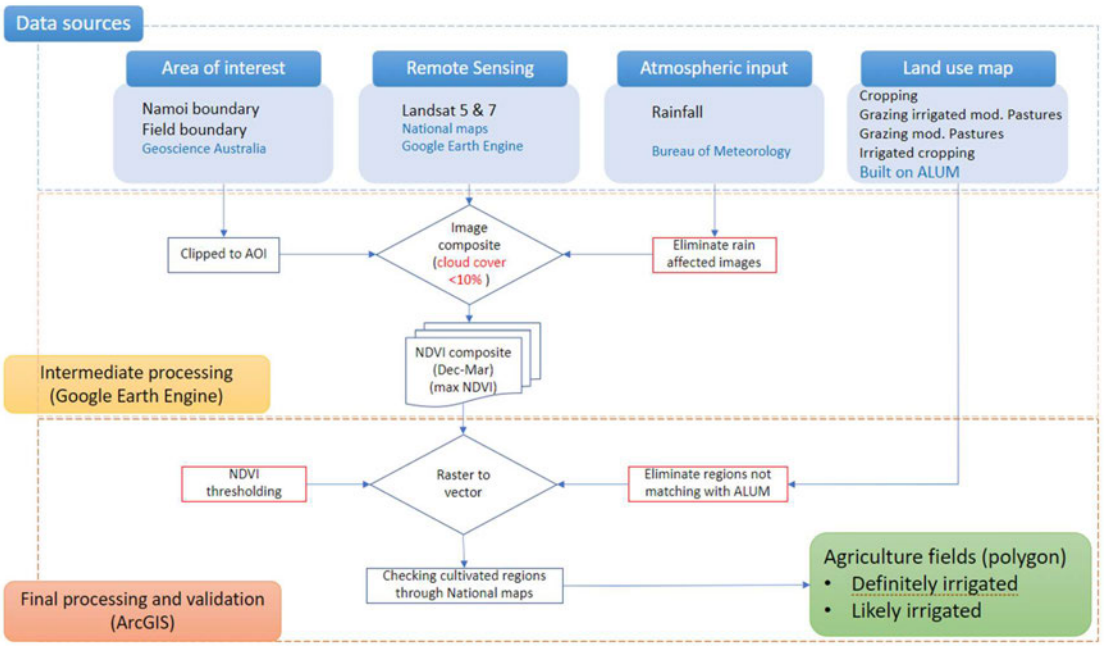

Figure 3: *Data sources and step wise data processing in Google Earth Engine and ArcGIS.*

2.3 Remotely sensed crop greenness assessment

The Normalised Difference Vegetation Index (NDVI) was selected by DPE and endorsed as the most suitable measure of canopy greenness, based on its sensitivity to plant canopy chlorophyll content (Colwell, 1974; Rouse et al., 1974; Shanahan et al., 2015; Tucker & Choudhury, 1987). Near-infrared (NIR, 0.85-0.89 µm) radiation used in the NDVI is scattered by the physical structure of the leaf, resulting in high levels of reflectance and transmittance, while the NDVI's red (0.63-0.69 µm) radiation is strongly absorbed by leaf pigments involved in photosynthesis (Blackburn, 2006; Daughtry, 2000; Jensen, 2021; Knipling, 1970). Planted crops exhibit significant changes in pigment concentration and structure as they develop from the early growing season through to maturity and senescence.

Such changes affect reflectance in NIR and red radiation, providing the theoretical basis to the NDVI in relating reflected radiation from satellite images to crop-specific growth patterns and optical signatures (including sowing, tillering, heading and maturity points), along with crop age and any crop stress (Nguy-Robertson et al., 2012). Therefore, a satellite based NDVI is increasingly used to monitor agricultural fields and as a tool to record crop phenological trends (Bhattarai et al., 2015; Ji et al., 2021; Katari et al., 2022; Liu et al., 2012; Pan et al., 2015; Yang et al., 2021; You et al., 2013).

Based on this evidence, the NDVI is assumed to be the correct indicator to represent summer season crop growth phenology in the Namoi region.

2.4 Data source overview & inputs assessment

Landsat-5 Thematic Mapper (TM, LT05) and Landsat-7 Enhanced Thematic Mapper Plus (ETM+, LE07) optical surface reflectance captured over the Namoi region in the summers of 1993-2000 was procured from Google Earth Engine (GEE) for the purpose of calculating a NDVI composite. Landsat-7 images were used only for 1999-2000 due to an unavailability of Landsat-5 images during that time. Using composite (repeat) observations increases the chance to get cloud-free data, increases the coverage of crop cycles, and increases the reliability of statistical data compared to a single observation (Gómez et al., 2016). The Landsat surface reflectance data available on GEE are orthorectified and corrected for solar angle (USGS SR product guide).

The Landsat data (and end outputs) were checked against data and images sourced through the *NationalMap*, which is an online map-based tool that allows easy access to spatial data from Australian Government agencies. It is managed by Geoscience Australia, in collaboration with CSIRO's Data61 for software development and data management (see https://nationalmap.gov.au/). It has gone through pre-processing steps including radiometric correction, geometric correction, and cloud removal (Li et al., 2010, 2012), which makes it suitable for determining irrigated crop areas. Landsat-5/Landsat-7 False Colour Composite (FCC) images and Landsat-5/Landsat-7 NDVI images were obtained from the *NationalMap* for the purposes of visual interpretation and comparison in deriving outputs.

Within the Namoi valley, there are 375 landholder property extents. The property extent input file contains polygon boundaries representing various agricultural regions with independent identification numbers.

Rainfall data for the study period were obtained through the nearest BOM rainfall station regions in the Namoi valley – Wee Waa (Lower Namoi) and Boggabri (Upper Namoi). These regions include five rainfall stations – 053044 (Wee Waa, George St), 053034 (Wee Waa, Pendennis), 055007 (Boggabri Post Office), 055044 (Boggabri Retreat) and 055268 (Boggabri Be-Bara). These stations provide continuously measured data for the study period and have been verified for accuracy by DPE.

The Land Use / Land Cover (LULC) produced by DPE was used to validate and mask yearly irrigated cropping regions identified through crop season NDVI composites. Based on information from Australian Land Use and Management (ALUM), aerial high-resolution stereo images, and field knowledge (about, for example, irrigation infrastructure), this provides the best available land use information for the Namoi region and the versions prepared in 2004, 2013, 2017 and 2022 are publicly available. For this study, the LULC version from 2004 was used because it was the nearest available date to the study time.

Table 1. Data input and source/custodian summary used in the Namoi DPE assessment.

Data Input	Source / Custodian
Imagery (Landsat-5 Thematic Mapper (LT05) and Landsat-7 Enhanced Thematic Mapper Plus (LE07)))	'NationalMap' (Australian government agencies, managed by Geoscience Australia in collaboration with CSIRO's Data61) Extraction Platform: Google Earth Engine
Rainfall (5 stations)	Bureau of Meteorology (BOM)
Namoi Property boundaries (375)	DPE (and Geoscience Australia)
Land Use / Land Cover (LULC) (2004)	Australian Land Use and Management (ALUM)
Evapotranspiration (ET)	METRIC EEFLUX (energy balance) Extraction Platform: Google Earth Engine

2.5 Study period and data driven assessment

Remotely sensed observations and climate data obtained for each summer season (December to March) between 1993/1994 and 1999/2000 were used in this analysis. Summer season observations were considered ideal to identify irrigated agriculture fields (Furby et al., 2008; Thomas, 2001) for three reasons:

1. **This is the growing season for irrigated crops.** It represents the complete life cycle of the irrigated summer season crops in the Upper and Lower Namoi. The sowing of most crops generally starts from early October and continues until the end of December, and harvesting generally starts at the end of February but may extend into mid-April (Rodriguez et al., 2011; Sacks et al., 2010). The major irrigated crop of the region is cotton, where the summer season (December to March) represents the entire cotton growth life cycle; from germination to flowering to maximum boll size or open boll (Tennakoon & Milroy, 2003). Other crops in rotation with cotton during the summer months are wheat, grain sorghum, barley, oilseeds, and grain legumes (Cooper, 1993). The summer season is therefore an ideal time to pick the optical signal specific for a crop (optical signature), which is critical in identifying irrigated crop areas in relation to other land uses.

2. **This is the season of peak growth for irrigated crops.** It is when crops require maximum water intake (Callan et al., 2004), allowing the capture of remotely sensed water stress signals due to insufficient water in non-irrigated crop areas (Ballester et al., 2019; Govender et al., 2009; Tilling et al., 2007). This is based on previous observations that water-stressed (non-irrigated) crops have significantly different canopy reflectance as compared to irrigated, non-stressed crops (e.g., maize and wheat – Aparicio et al., 2000; Tilling et al., 2007; Wardlow & Egbert, 2008).

3. **There is a higher chance of getting cloud-free optical satellite observations** (Ju & Roy, 2008).

3 The manual processing step as implemented by DPE (step by step)

The cloud-based Google Earth Engine (GEE) geospatial system was used for processing Landsat remote imagery to produce summer season NDVI composites (Gorelick et al., 2017). Following that initial processing in GEE, the ESRI ArcGIS standalone desktop system was used to estimate NDVI thresholds that were applied to identify irrigated crop areas. The result of inferred irrigated crop property boundaries was spatially overlapped and visually checked by DPE using Land Use / Land Cover (LULC) (ver. 2004) and the *NationalMap* to eliminate wrongly identified crop regions.

The following is a detailed explanation of each step.

Step 1: NDVI composite estimation process (covering cloud cover and rainfall factors)

Executing JAVA and/or Python script in Google Earth Engine (GEE) enabled the identification of all the Landsat-5 TM observations covering the summer season (December to March). Within each ROI, the cloud coverage threshold used was less than 10%.

Cloud cover reported by Landsat was considered in the processing. This is for the entire Landsat pass – i.e., for the entire field of view (Irish, 2000; Irish et al., 2006), which is much larger than the study area and does not necessarily represent the same cloud interference for each specific property extent.

A method that can identify cloud cover for a specific masked region or equivalent factor that mitigates the impact of cloud fraction was embedded in the code to reduce the chances of incorrect selection of cloud-affected observations (refer to Enhanced scripted method 5.2). An example is shown in Figure 4.

Figure 4. *Examples of Google Earth Engine Landsat 5 imagery of Lower Namoi region in Summer 1993/94, (left) without cloud filtering, (right) with 20% cloud filtering.*

The next consideration was eliminating all the images after a major rainfall event that occurred within the study area. This used two rainfall regions – Wee Waa (Lower Namoi) and Boggabri (Upper Namoi) – and was required because:

- Rainfall events could result in unexpected increases in canopy greenness. In the Namoi valley, this could create artifacts in growth NDVI signal patterns (Wang et al., 2003). This effect is likely due to the positive correlations between the NDVI and water availability following rainfall (Aguilar et al., 2012; Wang et al., 2003). There is a time lag between NDVI response and rainfall, which is lower in a dry period than in a wet period, where it can take up to one month to diminish the NDVI signal impact (Wang et al., 2003).

- The presence of cirrus clouds during these events which sometimes remains undetected by cloud removing algorithms (Alvarez-Mendoza et al., 2019; Qiu et al., 2020; Zhu et al., 2015) and which could mislead NDVI signal.

- Recent rainfall and water droplets on the crop canopy can interrupt the NDVI signal, increasing error in NDVI values.

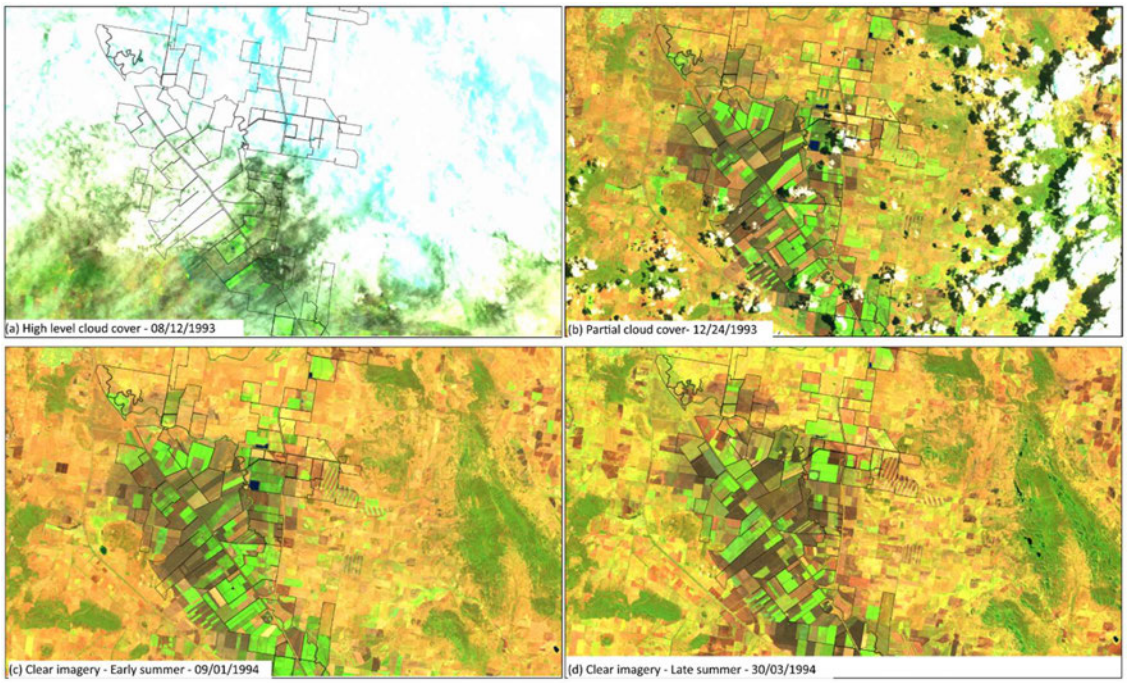

Figure 5. *Examples of Landsat 5 images for the Upper Namoi: (a) high level of cloud cover, (b) partial cloud cover, (c) and (d) clear imagery taken in early and late summer, respectively (from 'NationalMaps' by Geoscience Australia, viewed with False colour Green SWIR NIR).*

This elimination step required a manual check to see how many days the green area of the Landsat images was affected after rainfall events, so it could again be a potential source of error. The Landsat images were then cropped to the ROI using the Namoi property outlines. After going through the above manual selection steps, the NIR (0.85-0.89 µm) and RED (0.63-0.69 µm) reflection bands from the remaining Landsat images in the composite were used to calculate per pixel NDVI values.

A more robust and systematic method that can identify and minimise the impact of rainfall events on NDVI signal during the summer season would be considered an enhancement to this method (refer to Enhanced scripted method 5.3).

Step 2: MAX NDVI composite finalisation

Within GEE, the maximum NDVI raster values of the composite (Equation 1) were used to construct the final NDVI image for the cropping season (December – March) of a focus year.

$$NDVI_c = max(NDVI_1, NDVI_2, \dots \dots . NDVI_n) \quad (1)$$

where $NDVI_c$ represents maximum NDVI composite, while n represents the number of images available for a season (December to March).

Using the maximum NDVI during the cropping summer season was considered an accurate approach to detect irrigated crop areas (Pervez & Brown, 2010; Shahriar Pervez et al., 2014) because:

- This method captures the highest canopy pigmentation concentration, highest biomass, and densest vegetation cover achieved during the whole growing season (Paruelo et al., 2001; Wilson & Meyers, 2007). It is assumed that NDVI is directly correlated with crop canopy chlorophyll concentration (Shanahan et al., 2015; Tucker & Choudhury, 1987).
- Irrigated crops exhibit higher maximum NDVI than non-irrigated crops (Aparicio et al., 2000; Wardlow & Egbert, 2008), and the peak in NDVI during a dry season for any agricultural crop is a result of consistently adequate soil moisture that can only be a result of irrigation (Pervez & Brown, 2010)
- Some crops are cultivated and harvested within a very short period, such as the lucerne life cycle in the Namoi region, which is only from December to January.
- The classic maximum value composition (MVC) is the simplest way of interpolating temporal NDVI signals. It minimizes cloud contamination, ensures near-cloud-free wall-to-wall coverage, and minimizes sun-angle and shadow effects while reducing directional reflectance and off-nadir viewing effects (Cao et al., 2018; Holben, 1986).

The resulting maximum NDVI composite map was exported as a raster file to further process in ArcGIS.

Step 3: NDVI thresholding and manual check (iterative) process

The final NDVI raster for the focus year generated from Google Earth Engine was imported to ESRI's ArcGIS together with the Land Use / Land Cover (LULC) spatial layers to identify the satellite-based irrigated crop area. This processing step in ArcGIS ArcMap (or ArcGIS Pro) was done manually.

In the NDVI raster, each pixel is considered as a mixture of two classes, namely cropping and non-cropping land use. In distinguishing the pixel land use, it is necessary to select a threshold value and then assign pixels to one of the two classes based on whether their value is above or below the threshold. However, choosing an appropriate threshold value for NDVI can be challenging, as there is no threshold that works well across all years and all ROI's. This is because the optimal threshold for NDVI depends on a variety of factors, including the vegetation types, crop maturity, soil moisture, and atmospheric conditions (Nguy-Robertson et al., 2012; Wang et al., 2003; Wilson & Meyers, 2007).

To address this issue, it is often necessary to consider a range of threshold values for NDVI, which is often selected based on an image histogram or mean and standard deviation in observed NDVI of an image (e.g., Gong, 1993; Mas, 1999; Pu et al., 2008; Ridd & Liu, 1998; Singh, 1989). In this application, the possible threshold range for NDVI was calculated as:

$$NDVI\ threshold\ range_y = \overline{NDVI_y} + \sigma_y(0.25 - 0.75) \quad (2)$$

where $\overline{NDVI_y}$ and σ_y are the average NDVI value and standard deviation of the final NDVI raster for the year *y*.

Referring to the Equation 2, the value range of 0.25 – 0.75 was derived and adopted by the DPE Remote Sensing / Spatial team as an acceptable threshold range within the Namoi region to improve the accuracy of irrigatable crop area classification. This range is within the common NDVI range for Australian vegetation, e.g., about 0.1 to 0.7 (Bureau of Meteorology, 2023), 0.665 ± 0.044 for mangroves and saltmarshes, and 0.685 ± 0.054 for forested wetlands, 0.669 ± 0.067 for dunal wetlands, and 0.565 ± 0.095 for coastal swamps (Akumu et al., 2010).

This range was set to:

- Cover the maximum possible irrigated crop types while avoiding outliers (non-irrigated crops, natural crops and background information like soil and water) with visual interpretation.

- Cover the maximum possible crops under different climate conditions, including heatwaves, light cloud coverage, and fluctuations of soil moisture.

This threshold range was then tested using a laborious manual and time-consuming trial-and-error technique to determine the best threshold value for the particular year in focus.

First, the smallest NDVI value in the threshold range was used for initial thresholding, where pixels with NDVI values higher than the NDVI threshold were considered 'irrigated crop' vegetation. A raster layer of crop area corresponding to the lowest NDVI threshold was generated.

Step 4: Determining irrigated crop area (by property)

This deterministic process involved three main sources:

(i) Land Use Land Cover (LULC) (ver. 2004) spatial layer.
(ii) Visual interpretation (manual checking using Landsat images) and,
(iii) Evapotranspiration (ET), a numeric raster scale that measures the loss of water from both plants and the soil; needed for years with consistently high moisture for over 2 months.

The raster layer of irrigated crop area was vectorised to polygon areas of irrigated crop, which were compared to the Land Use Land Cover (LULC) (ver. 2004) spatial layer. This assumed that the irrigated cropping polygons from LULC in 2004 covered all irrigated cropping areas in the study year (between 1993/94 and 1999/2000). Regions (sections of polygons) considered outside of the LULC irrigated cropping area were eliminated from the end result.

The properties were then manually checked against the individual Landsat images (national scale during the 4-month cultivated period) to identify if these regions were 'true' irrigated cropping areas (i.e., appeared green at different shades during the period, looking like cropping fields). Those that did not look like cropping areas were manually eliminated.

In relation to using orthophotos to verify irrigated crop areas (using the NDVI threshold estimation method), it is worthwhile to note (for future reference) that DPE used Landsat for 2015 and earlier but Sentinel for 2016 and later, with the same workflow. As the request for floodplain harvesting purposes was from 1993 to 1999, DPE only used Landsat orthophoto imagery.

The manual refinement and iterative nature of this step was in reviewing the NDVI threshold used, which ultimately creates the irrigated crop area extent. At this step, the NDVI minimum threshold was increased within the NDVI threshold range (Equation 1) to find the highest possible NDVI threshold range that detected the 'true' cropping area. On average for the Namoi region, the DPE spatial team reported this to be within the 0.66 to 0.73 NDVI threshold range. This was repeated manually for each property, until the NDVI threshold range produced an accurate identification of irrigated crop area (for the study year in scope).

DPE then classified these areas into two categories:

(1) **Definite Irrigated Crop,** which fashioned regular shapes and continuously presented for a whole month. DPE's existing method involved using all three forms of assessment (as explained above), where definite areas would be returned if all three forms provided a correct alignment with LULC, visual interpretation and ET confirmation (if needed).

(2) **Likely Irrigated Crop**, which required another cross-check against the Landsat images (as detailed above). In DPE's existing method, likely areas would be returned if two forms provided a correct alignment with either LULC, visual interpretation and ET confirmation (if needed). For example, visual interpretation and ET may not always align with LULC, where this usually aligns with dryland crops (and sometimes dryland cropping can be turned into an irrigated crop area).

Step 5: Iteration across defined time-period

The whole workflow (as detailed from Step 1 to 4) was repeated for each year during the study period from 1993/94 to 1999/2000. Figure 6 and 7 show examples across the Lower and Upper Namoi of detected irrigation crop areas for two summer cropping seasons (1993/1994 and 1999/2000).

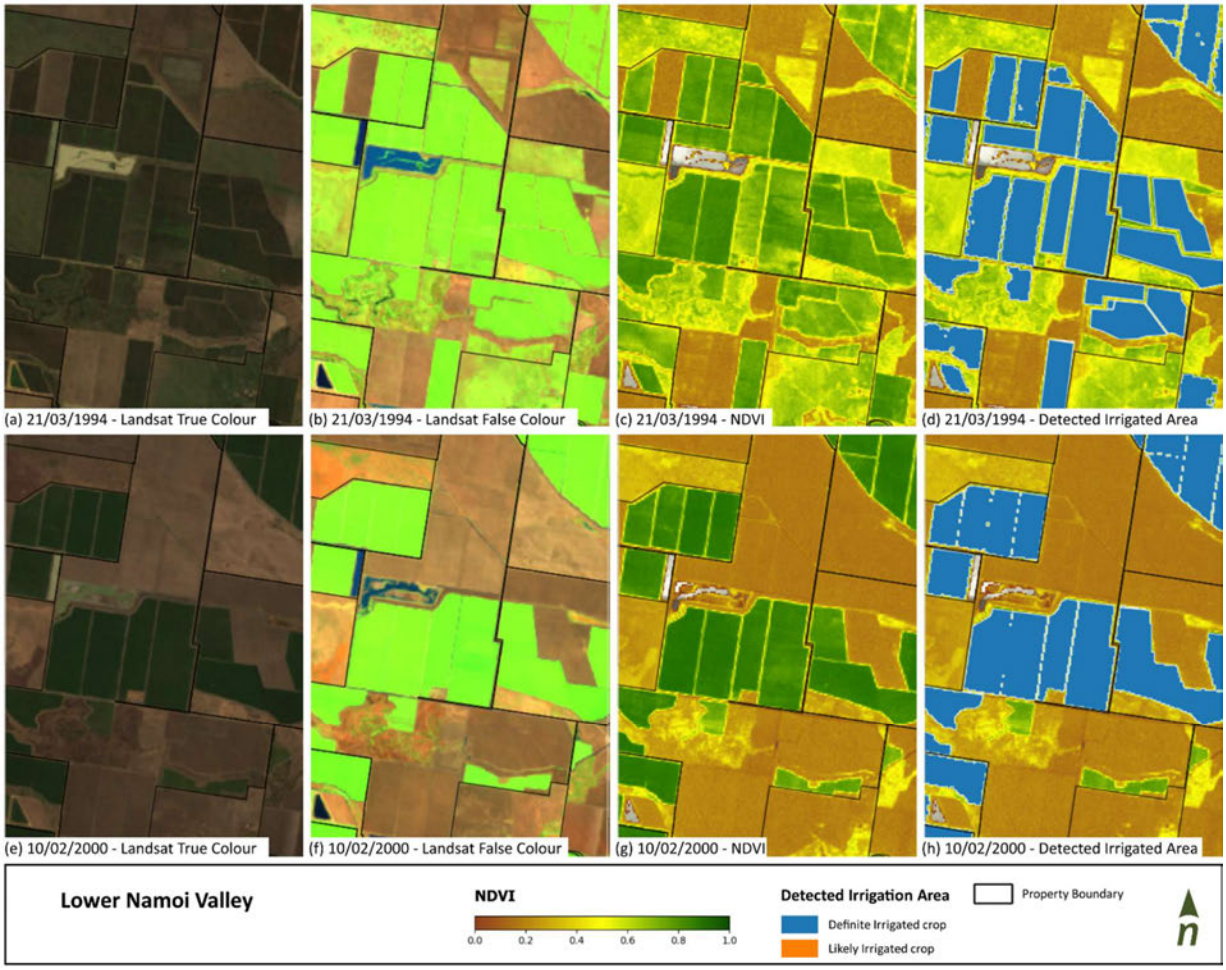

Figure 6. *Examples of detected irrigation crop areas for the summer cropping season in the Lower Namoi for 1993/1994 (top panel) and 1999/2000 (bottom panel). Columns from left to right: (a & e) Landsat True Colour, (b & f) Landsat False colour (Green, SWIR, NIR), (c & g) Landsat NDVI, and (d & h) detected irrigation cropping area. Landsat imagery was obtained from 'NationalMaps', Geoscience Australia.*

Figure 7. *Examples of detected irrigation crop area for the summer cropping season in the Upper Namoi for 1993/1994 (top panel) and 1999/2000 (bottom panel). Columns from left to right: (a & e) Landsat True Colour, (b & f) Landsat False colour (Green, SWIR, NIR), (c & g) Landsat NDVI, and (d & h) detected irrigation cropping area. Landsat imagery was obtained from 'NationalMaps', Geoscience Australia.*

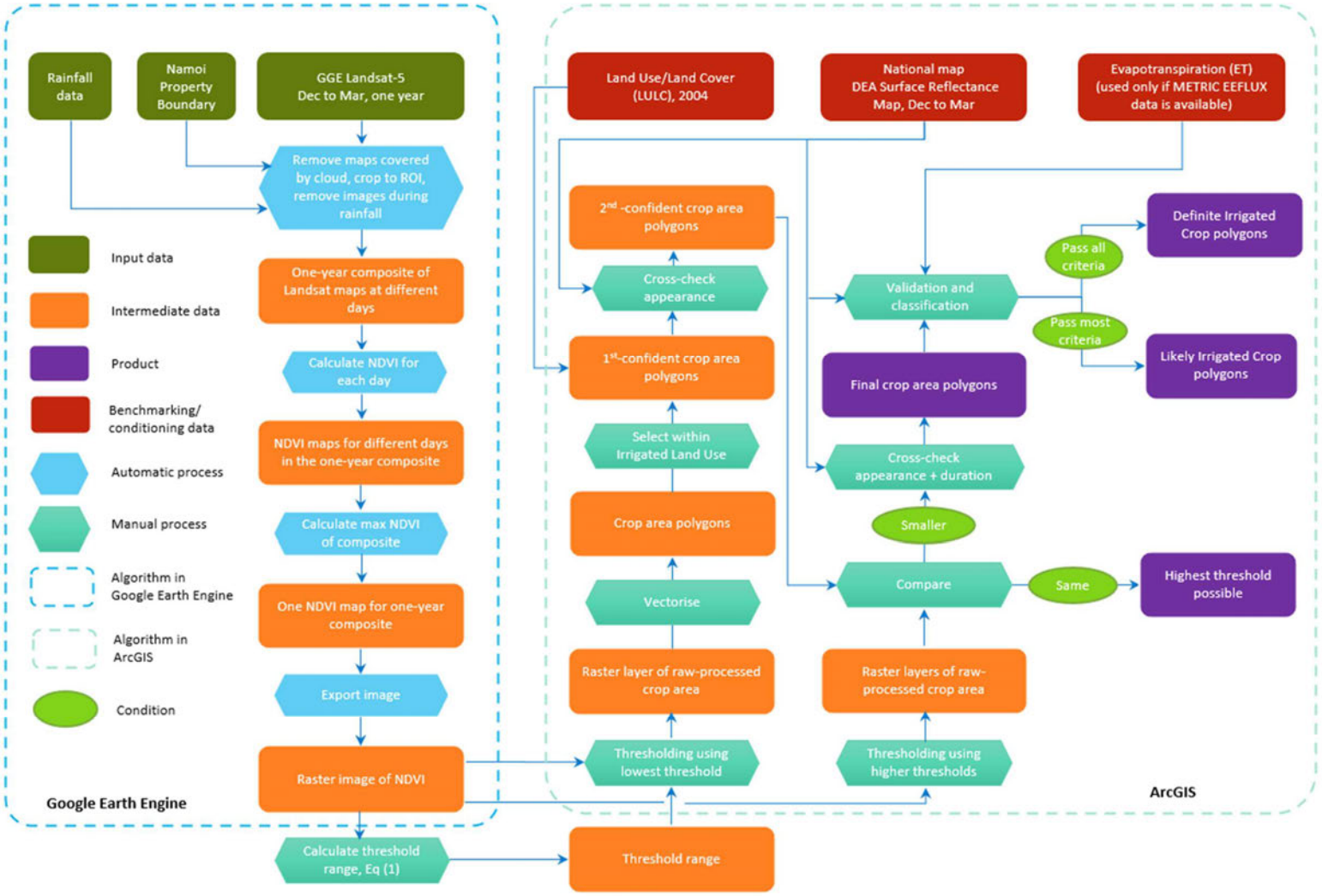

Figure 8. *DPE's end-to-end workflow (detailed information within steps)*

4 Automated (and objective) method detail

Alluvium has made process (automated) improvements on the current method of determining irrigated crop area mapping. The automation built into these improvements provide a more easily repeatable workflow that manages time and increases flexibility through iterative running, at both the valley and property scale.

4.1 Automating the Normalised Difference Vegetation Index (NDVI) threshold process

Manually setting the NDVI thresholds is subjective and time-intensive, requiring cumbersome manual checks against referenced layers (Furby et al., 2008). The automated and objective workflow has provided the following inclusions:

- Applying image corrections or conditions prior to setting thresholds, to reduce the difference in NDVI values due to terrain illumination and atmospheric (e.g., cloud) conditions (Drori et al., 2020; Furby et al., 2008; Mayaux et al., 2004).
- Smoothing NDVI time profiles by normalising the NDVI range in each image to a standard range, such as from a bare soil average NDVI value to a fully vegetated NDVI value (Mayaux et al., 2004; Shahriar Pervez et al., 2014).
- Incorporating more constraint conditions and indexes to the thresholding process (i.e., a decision tree), including temperature, time-integrated NDVI, and leaf area index (LAI) (Shahriar Pervez et al., 2014; Wilson & Meyers, 2007).
- Applying masks (e.g., for known irrigated areas and waterbodies) before setting thresholds to reduce the ambiguous NDVI values (Furby et al., 2008; Shahriar Pervez et al., 2014).
- Automatic thresholding to match calibrated datasets, including high-resolution satellite images (e.g., Ikonos) and known irrigated areas (Furby et al., 2008; Shahriar Pervez et al., 2014). The thresholding sets can be constructed separately for wet years and dry years, given that the NDVI of a wet year is higher than a dry year for the same region (Aguilar et al., 2012; Wang et al., 2003).

4.2 Minimising the impact of cloud-affected areas on NDVI

Image cloud masking (per pixel review) is now included to identify:

- Cells of dark pixels (cloud shadow).
- Cells of cloud presence (cloud cover).
- Cells of cloud detection (cirrus cloud formations).

An example image showing all three of these cell types is shown in Figure 9. Applying this quality assurance (QA) to each daily Landsat-5 (TM)/Landsat-7 (ETM+) image excludes (or ‘masks out') only their cloud-impacted pixels rather than removing the whole image (an example is shown in Figure 10). The positive retention of image cell values across a summer season enhances the statistical distribution of daily NDVI signals, which is an important consideration when completing the maxNDVI composite image.

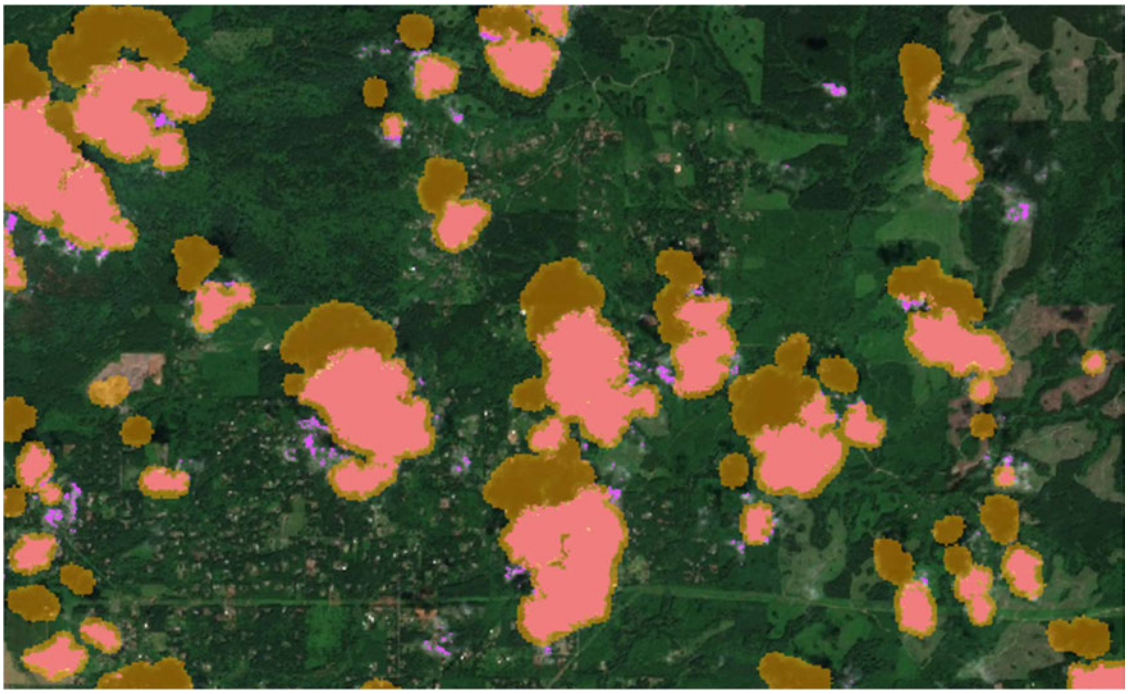

Figure 9. *Landsat 5-TM showing cloud shadow (brown), cloud presence (pink) and cloud detection (purple).*

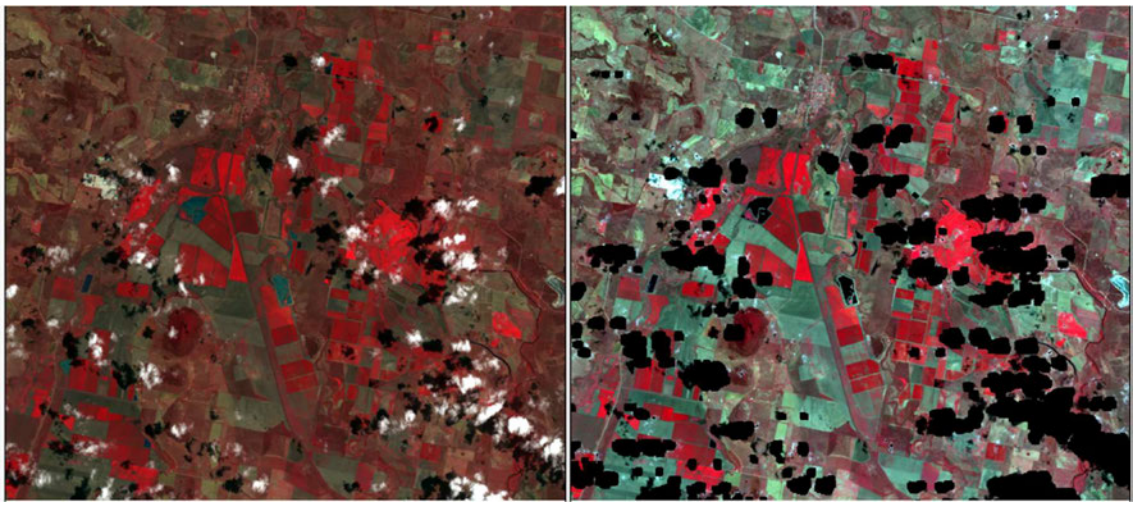

Figure 10. *Landsat 5-TM raw image from 24th March 1998 showing cloud (left) and Google Earth Engine scripted properties to remove cloud shadow, presence, and detection (right).*

4.3 Minimising impact of rainfall events on NDVI

Significant rainy days were identified as days representing more than 15% of rainfall during a given summer (December to March), as recorded at all five BOM rainfall stations (introduced in Section 2.4). Through analysis of different storm events and properties, it was determined that it takes 15 days after one of these significant rainfall events for NDVI signals to return to pre-rainfall conditions.

Our enhanced method considered the rainfall coverage across both the Upper and Lower Namoi, and we subsequently included two extra rainfall stations – Curlewis Post Office (055014) and Breeza (Alpha) (055275) – in the calculation of the maxNDVI composite from GEE.

Accounting for the impact of rainy days on NDVI images involved two methods, both implemented in the enhanced scripted workflow:

1) Identifying significant rainy days during a season (December to March) and excluding the nearest Landsat image from the maxNDVI composite calculation. Landsat dates excluded were within 15 days of the identified rainy days. This number of days can be changed in the scripted workflow to suit any alteration DPE requires, and all the available Landsat dates representing significant rainy days can be seen while the script is running.

2) Masking NDVI pixels that resulted from a difference in the NDVI signal of +0.2 or -0.2 of the forthcoming NDVI date. Theoretically, this method not only accounts for significant rainfall events but also can eliminate the impact of heat stress on the irrigated crop areas. The NDVI signal range (e.g., +0.2 or – 0.2 of the previous baselined NDVI signal) can be changed in the scripted (automated??) workflow as required by DPE.

The scripted workflow has been set up so that these two methods can be run in parallel or individually. Our recommendation is to use both methods, as this provides a cohort range to define irrigated crop areas within each property.

The remaining NDVI pixels and dates, after accounting for the rainfall and cloud impacts, can be used to calculate maxNDVI for each summer season. All the images including the raw Landsat, the cloud mask Landsat, and the maxNDVI composite can be exported as an image collection (.tif) to Google Drive.

4.4 Minimising impact of heat waves on NDVI

Drought stress is often caused by a combination of low water availability and increased temperature. As described above in relation to rainy days, the enhanced method now masks the NDVI pixels that were the result of a difference within -0.2 to 0.2 of the forthcoming NDVI date. This has mitigated the impact of heat waves (drought stress) on each daily NDVI signal. If this were not accounted for, the impact of heat stress and the subsequent fluctuation in the NDVI signal could affect the calculation of the NDVI composite image for each year's summer season.

4.5 Applying Landsat-5 (TM)/Landsat-7 (ETM+) image scale (rescaling) factor

Landsat Collection 2 Surface Reflectance measures the fraction of incoming solar radiation that is reflected from Earth's surface to the Landsat sensor. Surface reflectance improves comparison between multiple images over the same region by accounting for atmospheric effects such as aerosol scattering and thin clouds, which can help in the detection and characterization of Earth surface change (USGS Landsat program requirements).

A scale factor must be applied to both Collection 1 and Collection 2 Landsat Level-2 surface reflectance and surface temperature products before using any Landsat data (USGS). Landsat Collection 1 and Collection 2 level-2 science products have different scaling factors, fill values, and are different data types. Landsat Collection 2 surface reflectance has a scale factor of 0.0000275 and an additional offset of -0.2 per pixel. For example, a pixel value of 18,639 is multiplied by 0.0000275 for the scale factor, and then -0.2 is added for the additional offset to get a reflectance value of 0.313.

4.6 Automating the NDVI threshold process

The automated method has involved an automated script retrieving the following from the observed maxNDVI composite, corresponding to each growing season and ROI:

- Actual mean maxNDVI value.
- Actual maxNDVI pixel count.
- Actual maxNDVI standard deviation.
- Simulated maxNDVI threshold value where the constant varies by 0.01 (between 0.25 and 0.75).

This is repeated for each individual ROI (a unique number within each of the 375 property names).

For the final output, the automated script determines an optimum criterion that determines, for each ROI, the modelled maxNDVI value and corresponding pixel count (irrigated crop area). The optimum (highest) ratio is calculated as the pixel count (area) **within** each ROI, relative to the pixel count (area) **outside** of each ROI; but conditionally inside DPE's identified irrigated property boundary and LULC. As noted above, the spikes in NDVI (or "green flush") immediately post rainfall events has been mitigated by the detail provided in section 4.3.

For each of the 375 property extents within the Namoi valley, a comparison of the enhanced method with the existing DPE method was performed based on the final maxNDVI value and corresponding irrigated crop area. An observation was that both the LULC type (e.g., cropping, grazing modified pasture or irrigated cropping) and properties used for cropping vary depending on the year (e.g., 305 properties in 1993/94, compared to 313 properties in 1994/95).

5 Enhanced scripted workflow – summary of the three modules

The end-to-end python GIS workflow has been divided into the three key modules summarised below. Each module needs to run separately, one after another. For the script to run successfully, four things need to occur:

(A) Save the "Script_Input" locally – this contains rainfall, properties, LULC, and Module 2 dependencies.
(B) Install all the essential python libraries as imported in each of the programming modules.
(C) Edit the code to allocate an "INPUT_PATH".
(D) Edit the code to allocate an "OUTPUT_PATH".

Module 1: Construct an NDVI composite from Google Earth Engine (GEE)

- Runs cloud masking, so that only contaminated pixels are removed rather than the whole image.
- Imports the Namoi ROI input file (375 properties across the Upper and Lower regions).
- Selects Landsat summer images corresponding to crop seasons (e.g., 1993-12-01 to 1994-03-31, for "season=1994").
- Creates a maxNDVI composite using the filtered images/pixels and exports it to a user-defined location.
- Uses rainfall information from all seven BOM stations (it is also possible to use only the nearest station).
- Completes two methods, in parallel, that identify rain-impacted days in NDVI images (as section 4.3).
- Downloads each image (raw Landsat images, cloud masked Landsat images, and a maxNDVI composite) to your drive for verification and validation.

Module 2: Simulate the NDVI threshold and choose the optimal ROI-specific threshold and constant

- Generates NDVI thresholds according to Equation 2, by varying the constant value (0.25 – 0.75) starting from 0.75 with a decrement of 0.10. We also trialled a decrement of 0.01 but the change in output was not significant enough to justify the computing time and cost.
- Calculates "pixel ratio 1", which is the ratio of cells of the NDVI composite that are "inside property pixels" and those cells "outside property pixels". A ratio close to 1.0 reflects the optimal NDVI threshold and constant when aligned to the ROI property boundary.
- Calculates "pixel ratio 2", which is the ratio of cells of the NDVI composite that are inside and outside of LULC-defined irrigated fields ("outside LULC pixels" and "inside LULC pixels"). Conditionally, this ratio also includes cells within the selected ROI (reflecting the NDVI threshold and constant used). A ratio close to 0.0 reflects the optimal NDVI threshold and constant when aligned to the LULC layer.

  The script automates the process and provides the most accurate coverage of NDVI greenness pixels within property boundaries and optimally aligned to LULC (as above). Two elements were added and automated within the script for efficiency:
  (1) An upper (0.7) and lower (0.6) NDVI threshold were applied for consistency.
  (2) An area threshold of 0.5 ha was applied to remove the small and scattered cell aggregates not considered part of an irrigated cropping area. Both these values are flexible and can be changed if needed and rerun by DPE.

Module 3: Estimate crop area using optimal threshold and export results (raster & vector)

- Applies, for each summer season, the NDVI threshold and constant (from Module 2) to each ROI iteratively.
- Extracts the cell count and corresponding irrigated crop area (in hectares) for each property, in both raster image and vector format.
- Extracts a summary of the LULC classification, detailing the proportion of 'irrigated cropping', 'cropping' and 'grazing modified pastures'.

  This module also includes automation of some manual end tasks (e.g., intersecting and dissolving fragmented irrigated crop areas within property boundaries and eliminating small and scattered pixels).

6 Comparative output assessment (DPE vs Alluvium methods)

We compared the outputs of the existing DPE with automated Alluvium method across the 60 properties in the Namoi valley that are eligible for an unregulated floodplain harvesting (FPH) entitlement. Overall (at the valley scale), the Alluvium method produced a slightly higher (by 4.0%) irrigated crop area (102,256 ha using the automated method and 98,346 ha using the existing manual method).

Table 2. Descriptive statistics of the Alluvium and DPE methods for determining irrigated crop area (for 60 properties across six review years, from 1993/94 to 1998/99).

Irrigated Crop Area (Ha) - DPE method		Irrigated Crop Area (Ha) - Alluvium method	
Mean	273.2	Mean	284.0
Standard Error	14.0	Standard Error	17.7
Median	191.5	Median	186.8
Mode	0.0	Mode	0.0
Standard Deviation	265.2	Standard Deviation	335.5
Sample Variance	70,315.1	Sample Variance	112,578.6
Kurtosis	5.8	Kurtosis	15.9
Skewness	1.9	Skewness	3.3
Range	1,662.0	Range	2,610.2
Minimum	0.0	Minimum	0.0
Maximum	1,662.0	Maximum	2,610.2
Sum	98,345.7	Sum	102,255.8
Count	360.0	Count	360.0
Confidence Level (95.0%)	27.5	Confidence Level (95.0%)	34.8

A **confidence category** was assigned to each of the 60 properties, comparing the final irrigated crop area (ha) output from the two methods. The confidence category reflects the variance (average of differences) measured in irrigated crop area average across the six years (1993/94 to 1998/99). Four confidence categories were assigned, as below, including a count of property allocation:

- **Very High** (+ - 0 to 2 % variance) – 14 unregulated properties, 23% of total
- **High** (+ - 2 to 5 % variance) – 23 unregulated properties, 38% of total
- **Moderate** (+ - 5 to 10 % variance) – 18 unregulated properties, 30% of total
- **Low** (+ - > 10 % variance) – 5 unregulated properties, 8% of total)

Table 3 shows an assessment of the differences between the two methods, highlighting the properties that may need further scrutiny and review ('Moderate' and 'Low' confidence categories).

Overall, the two methods produced similar results, with 92% of the properties within 10%. Most (61%) of the 60 unregulated properties were even within 5% variance between the two methods.

Table 3. Irrigated crop area (ha) per property, showing a 6-year comparison variance between the DPE water and Alluvium methods. This table shows the following confidence factor categories: 'Very High' (+ - 0 to 2 %), 'High' (+ - 2 to 5 %), 'Moderate' (+ - 5 to 10 %) and 'Low' (+ - >10 %).

Property Name	6-year comparison variance	Confidence factor	Property Name	6-year comparison variance	Confidence factor
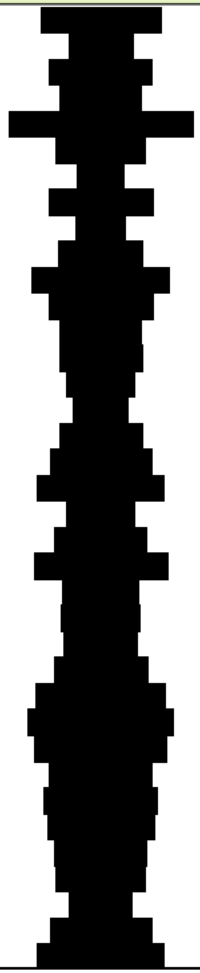	-1.0%	VERY HIGH	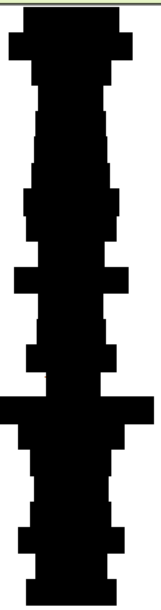	-6.2%	MODERATE
	0.5%	VERY HIGH		-5.1%	MODERATE
	-0.3%	VERY HIGH		-5.8%	MODERATE
	-0.6%	VERY HIGH		-8.4%	MODERATE
	-1.8%	VERY HIGH		-6.0%	MODERATE
	0.8%	VERY HIGH		7.2%	MODERATE
	-1.8%	VERY HIGH		-9.5%	MODERATE
	1.5%	VERY HIGH		7.5%	MODERATE
	-0.7%	VERY HIGH		-5.3%	MODERATE
	-1.6%	VERY HIGH		8.0%	MODERATE
	1.3%	VERY HIGH		-5.6%	MODERATE
	-1.3%	VERY HIGH		5.9%	MODERATE
	-0.6%	VERY HIGH		8.3%	MODERATE
	0.3%	VERY HIGH		-6.5%	MODERATE
	5.0%	HIGH		6.8%	MODERATE
	3.0%	HIGH		8.2%	MODERATE
	-4.8%	HIGH		-9.7%	MODERATE
	-3.2%	HIGH		5.7%	MODERATE
	4.6%	HIGH		13.2%	LOW
	-4.5%	HIGH		-43.0%	LOW
	2.4%	HIGH		-13.4%	LOW
	3.0%	HIGH		15.8%	LOW
	3.3%	HIGH		15.3%	LOW
	2.8%	HIGH			
	-4.8%	HIGH			
	-5.0%	HIGH			
	5.0%	HIGH			
	-3.2%	HIGH			
	2.1%	HIGH			
	2.7%	HIGH			
	2.3%	HIGH			
	-2.3%	HIGH			
	3.0%	HIGH			
	-2.6%	HIGH			
	-5.0%	HIGH			
	4.2%	HIGH			
	-2.4%	HIGH			

7 Summary of output (Alluvium automated workflow)

The final folder structure is organised around two sets of property type outputs (30 groundwater and 60 unregulated) for each of the six summer seasons (1993/94 to 1999/2000). These outputs include:

- A masked raster image of NDVI greenness extent for each property for each year, in the "roi_images" folder.
- An NDVI compositive image that mosaics each summer season, in the "roi_mosaics" folder.
- Cropping area spatial extents (by property), for all years, in the "vector_cropping_area" folder.
- An Excel file detailing (for each ROI and year) the actual and simulated irrigated cropping area, NDVI thresholds used, NDVI final optimal values, and cropping type summary (per year), in the "csv" folder.

8 NDVI and evapotranspiration (ET) as indicators of irrigated crop areas

Three test sites were supplied by DPE for the purpose of comparing irrigated crop areas from Normalised Difference Vegetation Index (NDVI) with DPE-supplied data on evapotranspiration (ET). The three sites were [redacted] in the Lower Namoi, [redacted] in the Upper Namoi, and the DPI Ag test site (comprised of [redacted] and [redacted]).

The three validation sites are a good representation of the Upper and Lower Namoi. Table 4 shows the property area (ha) and the irrigated cropping area determined by the Alluvium method, and Figures 12 to 14 are a visual comparison of ET and NDVI (using the Alluvium method) for each of the three sites in a single summer. They show that there is some correspondence between the two metrics in detecting the presence/absence of irrigated cropping areas.

However, the pixel-based regression statistics (Table 5) and relationship (Figure 14) between ET and NDVI for the three sites are relatively weak (r-squared = 0.22 and adjusted r-squared = 0.22). Furthermore, it is important to note that the NDVI presented in Figure 15 is a composite image using a full summer season (December to March), whereas the ET is from a single day. The data inputs for these statistics were point cell values where both NDVI and ET are present at the test sites (for [redacted] in 1993/94, [redacted] in 1998/99, and the DPI Ag test site in 1993/94).

It is recommended that the relationship between NDVI and ET be explored further with comparable and more extensive datasets. This would provide further insights into the relationship between the two metrics and the potential for them to be used as complementary indices for detecting irrigated crop areas. In future method refinements, we also recommend that data on actual irrigated areas be collected to build a dataset that can be used for independent validation.

Table 4. Property area (ha) and irrigated cropping areas determined by the Alluvium method for summer seasons between 1993/94 and 1999/2000.

					Irrigated Cropping area, Ha (Alluvium method)						
ET Test Validatio	EOI_Unique	EOI_Numberroperty_Narroperty_Area_			1993/94	1994/95	1995/96	1996/97	1997/98	1998/99	1999/2000
Upper Namoi	[redacted]	[redacted]	[redacted]	1,115.9	254	327	358	293	314		247
Lower Namoi				2,680.9	553	771	1056		121	816	560
				246.5				1	1		1
				0.4							
				1,123.5	289	373	360	488	366		420
DPI Ag test site				29.9							
				132.4	52	30	67	21		6	69
				587.0	248	194	274	193	263		202
				486.3	218	123	167	123	216		217
				1,013.3	299	489	204	605	564		513

Figure 11. *Irrigated crop areas at the* [redacted] *site derived from ET data (top) and the NDVI Alluvium method (bottom), both within the 1993/94 summer season.*

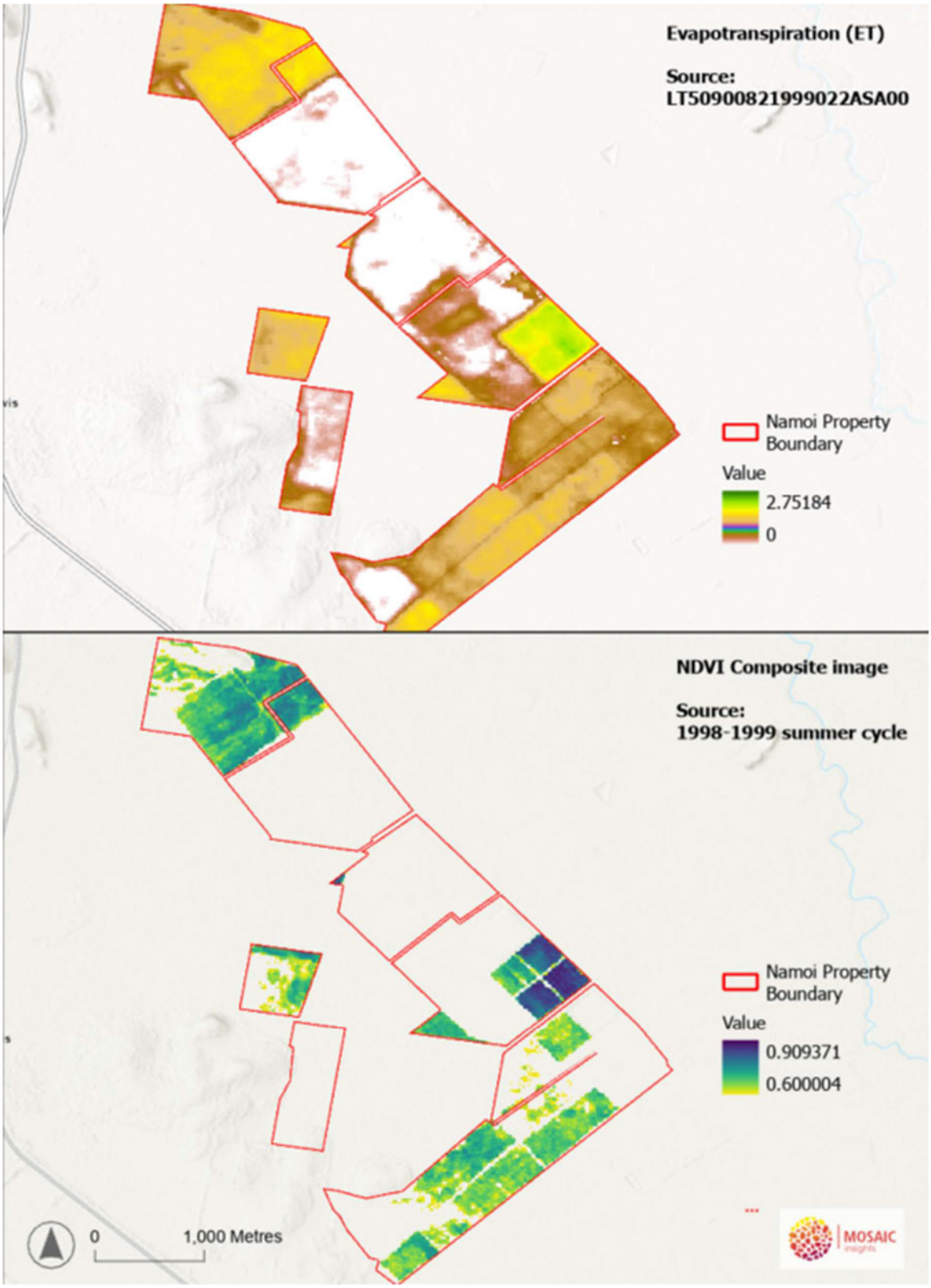

Figure 12. *Irrigated crop areas at the* [redacted] *site derived from ET data (top) and the NDVI Alluvium method (bottom), both within the 1998/99 summer season.*

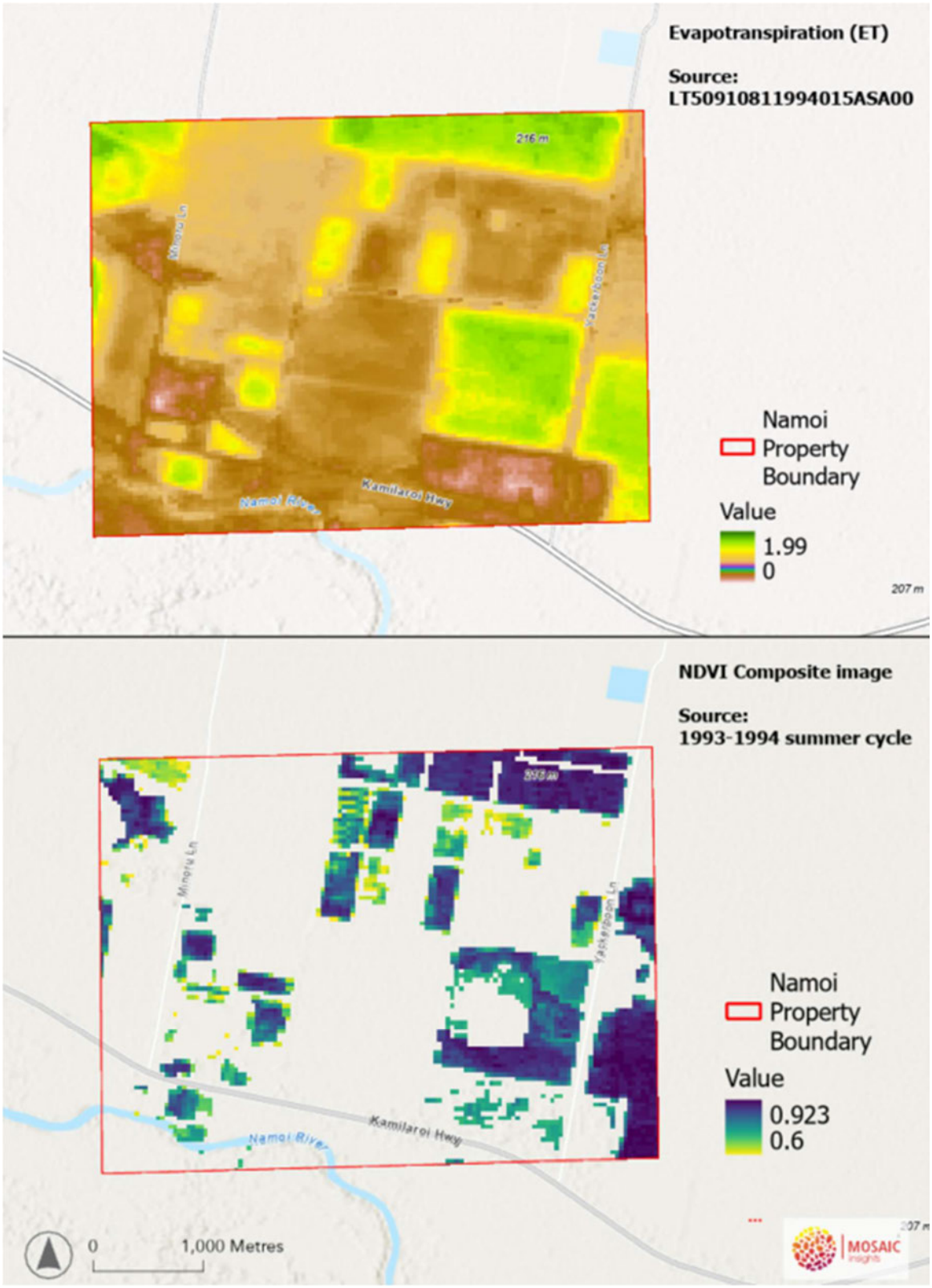

Figure 13. *Irrigated crop areas at the [redacted] (comprised of [redacted] and [redacted]) derived from ET data (top) and the NDVI Alluvium method (bottom), both within the 1993/94 summer season.*

Table 5. Regression statistics for the relationship between evapotranspiration (ET) and Normalised Difference Vegetation Index (NDVI) at the three validation test sites.

Regression Statistics	
Multiple R	0.467
R Square	0.218
Adjusted R Square	0.218
Standard Error	0.130
Observations	37845

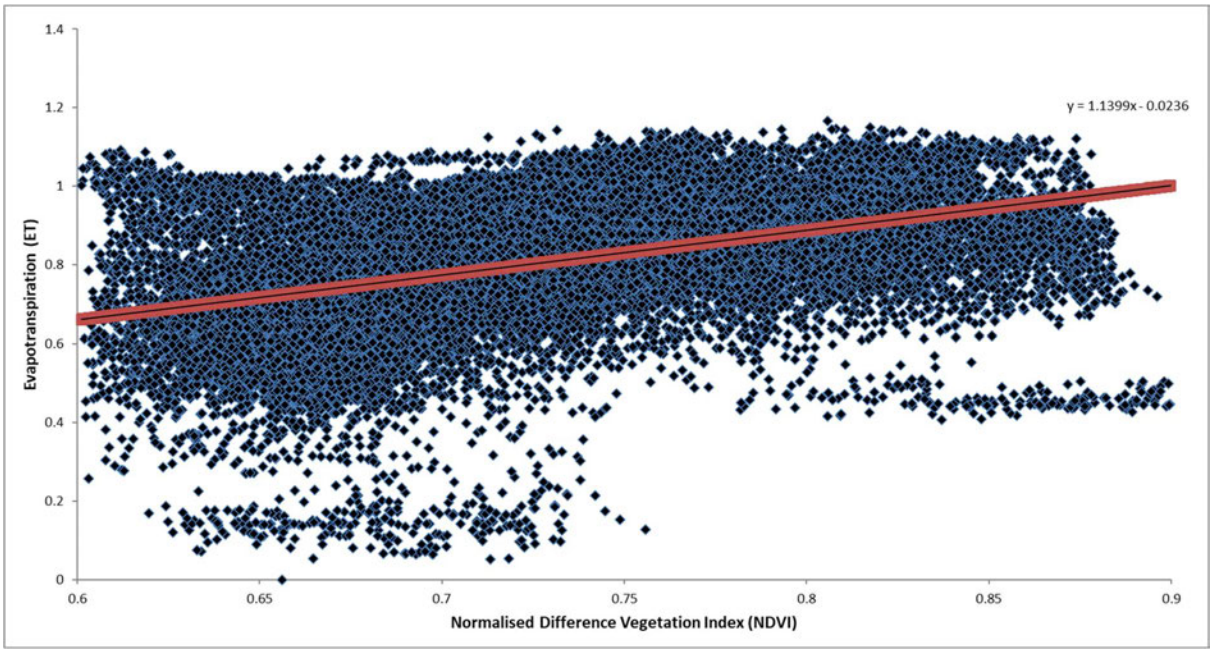

Figure 14. *Relationship between evapotranspiration (ET) and the Normalised Difference Vegetation Index (NDVI) at the three validation test sites, with a line of best fit (r-squared = 0.218, adjusted r-squared = 0.218).*

9 Conclusions

- The Normalised Difference Vegetation Index (NDVI), which was selected by DPE, is a method supported by scientific literature to correctly measure canopy greenness. It is based on sensitivity to plant canopy chlorophyll content and, to some extent, the canopy's photosynthetic activeness, and can be used to represent summer season crop growth areas.
- The summer season (December to March) is ideal to pick the optical signal specific for a crop (its optical signature), which is critical in distinguishing irrigated crop areas from other land uses.
- Alluvium's automated method provides DPE with the ability to quickly, easily and systematically calculate (and then repeat if necessary) the irrigated cropping area for any property in the Namoi valley.
- Whilst both the DPE and Alluvium methods have benefits (accuracy levels) and apparent errors [founded by the way processing and analysis is completed, i.e., subjective, and manual (DPE) vs objective and automated (Alluvium), the output from this project provides DPE with a spatial workflow that:
    - (i) Considered rainfall coverage and designed a systematic method to account for rainfall events on the NDVI signal.
    - (ii) Minimised the cloud impact on Landsat 5-TM images, by accounting for (but not completely removing) daily images with cloud shadow, cloud presence and cloud detection.
    - (iii) Mitigated the impact of heat waves (drought stress) on daily NDVI signals.
    - (iv) Optimised ROI-specific NDVI thresholds, constant values, property boundaries and LULC extents.
- At the valley scale, there was strong correspondence and a high level of confidence between the DPE and Alluvium methods, where 92% of the properties were within 10%. To achieve a highly accurate indicator at the property scale, it is recommended that DPE review the automated / scripted workflow and complete further refinement and accuracy investigation (such as an in-depth sensitivity assessment of specific parameters within the three python modules, outlined in Section 5).
- There appears to be a relationship between NDVI and ET when inferring irrigated cropping areas. It is recommended that this relationship be explored further with comparable and more extensive datasets.

10 References

Aguilar, C., Zinnert, J. C., Polo, M. J., & Young, D. R. (2012). NDVI as an indicator for changes in water availability to woody vegetation. *Ecological Indicators*, *23*, 290–300. https://doi.org/10.1016/j.ecolind.2012.04.008

Akumu, C. E., Pathirana, S., Baban, S., & Bucher, D. (2010). Modeling Methane Emission from Wetlands in North-Eastern New South Wales, Australia Using Landsat ETM+. *Remote Sensing*, *2*(5), 1378–1399. https://doi.org/10.3390/rs2051378

Alvarez-Mendoza, C. I., Teodoro, A., & Ramirez-Cando, L. (2019). Improving NDVI by removing cirrus clouds with optical remote sensing data from Landsat-8 – A case study in Quito, Ecuador. *Remote Sensing Applications: Society and Environment*, *13*, 257–274. https://doi.org/10.1016/j.rsase.2018.11.008

Aparicio, N., Villegas, D., Casadesus, J., Araus, J. L., & Royo, C. (2000). Spectral Vegetation Indices as Nondestructive Tools for Determining Durum Wheat Yield. *Agronomy Journal*, *92*(1), 83–91. https://doi.org/10.2134/agronj2000.92183x

Ballester, Brinkhoff, Quayle, & Hornbuckle. (2019). Monitoring the Effects of Water Stress in Cotton using the Green Red Vegetation Index and Red Edge Ratio. *Remote Sensing*, *11*(7), 873. https://doi.org/10.3390/rs11070873

Beck, H. E., Zimmermann, N. E., McVicar, T. R., Vergopolan, N., Berg, A., & Wood, E. F. (2018). Present and future Köppen-Geiger climate classification maps at 1-km resolution. *Scientific Data*, *5*(1), 180214. https://doi.org/10.1038/sdata.2018.214

Bhattarai, N., Quackenbush, L. J., Dougherty, M., & Marzen, L. J. (2015). A simple Landsat–MODIS fusion approach for monitoring seasonal evapotranspiration at 30 m spatial resolution. *International Journal of Remote Sensing*, *36*(1), 115–143. https://doi.org/10.1080/01431161.2014.990645

Blackburn, G. A. (2006). Hyperspectral remote sensing of plant pigments. *Journal of Experimental Botany*, *58*(4), 855–867. https://doi.org/10.1093/jxb/erl123

Bureau of Meteorology. (2021). *Climate statistics for Australian locations: Summary statistics Narrabri West Post Office Document*. http://www.bom.gov.au/climate/averages/tables/cw_053030.shtml

Bureau of Meteorology. (2023). *Map Information - Normalised Difference Vegetation Index*. http://www.bom.gov.au/climate/austmaps/about-ndvi-maps.shtml#:~:text=Vegetation%20NDVI%20in%20Australia%20typically,water%20bodies%20have%20negative%20values.

Callan, V., Christiansen, I., & Harris, G. (2004). *Knowledge management in cotton and grain irrigation* (3rd ed.). Australian Cotton Cooperative Research Centre.

Cao, R., Chen, Y., Shen, M., Chen, J., Zhou, J., Wang, C., & Yang, W. (2018). A simple method to improve the quality of NDVI time-series data by integrating spatiotemporal information with the Savitzky-Golay filter. *Remote Sensing of Environment*, *217*, 244–257. https://doi.org/10.1016/j.rse.2018.08.022

Colwell, J. E. (1974). Vegetation canopy reflectance. *Remote Sensing of Environment*, *3*(3), 175–183. https://doi.org/10.1016/0034-4257(74)90003-0

Cooper, J. L. (1993). *Rotopak - developing rotations to overcome soil degradation for irrigated cotton systems*.

Dalgliesh, N., Cocks, B., & Horan, H. (2012, October 14). APSoil-providing soils information to consultants, farmers and researchers. *Proceedings of the 16th Australian Agronomy Conference*.

Daughtry, C. (2000). Estimating Corn Leaf Chlorophyll Concentration from Leaf and Canopy Reflectance. *Remote Sensing of Environment*, *74*(2), 229–239. https://doi.org/10.1016/S0034-4257(00)00113-9

Donaldson, S., & Heath, T. (1997). *Namoi River Catchment : report on land degradation and proposals for integrated management for its treatment and prevention*. Department of Land and Water Conservation.

Drori, R., Dan, H., Sprintsin, M., & Sheffer, E. (2020). Precipitation-Sensitive Dynamic Threshold: A New and Simple Method to Detect and Monitor Forest and Woody Vegetation Cover in Sub-Humid to Arid Areas. *Remote Sensing*, *12*(8), 1231. https://doi.org/10.3390/rs12081231

Furby, S. L., Caccetta, P. A., Wallace, J., Wu, X., O'Connell, J., Chia, J., Collings, S., Traylen, A., & Devereaux, D. (2008). Continental scale land cover change monitoring in Australia using Landsat imagery. *Studying, Modelling and Sense Making of Planet Earth*.

Gómez, C., White, J. C., & Wulder, M. A. (2016). Optical remotely sensed time series data for land cover classification: A review. *ISPRS Journal of Photogrammetry and Remote Sensing*, *116*, 55–72. https://doi.org/10.1016/j.isprsjprs.2016.03.008

Gong, P. (1993). Change Detection Using Principal Component Analysis and Fuzzy Set Theory. *Canadian Journal of Remote Sensing*, *19*(1), 22–29. https://doi.org/10.1080/07038992.1993.10855147

Gorelick, N., Hancher, M., Dixon, M., Ilyushchenko, S., Thau, D., & Moore, R. (2017). Google Earth Engine: Planetary-scale geospatial analysis for everyone. *Remote Sensing of Environment*, *202*, 18–27. https://doi.org/10.1016/j.rse.2017.06.031

Govender, M., Govender, P., Weiersbye, I., Witkowski, E., & Ahmed, F. (2009). Review of commonly used remote sensing and ground-based technologies to measure plant water stress. *Water SA*, *35*(5). https://doi.org/10.4314/wsa.v35i5.49201

Green, D. L., Petrovic, J., Burrell, M., & Moss, P. (2011). *Water resources and management overview: Murrumbidgee catchment*.

Holben, B. N. (1986). Characteristics of maximum-value composite images from temporal AVHRR data. *International Journal of Remote Sensing*, *7*(11), 1417–1434. https://doi.org/10.1080/01431168608948945

Hope, M., & Bennett, R. (2002). *Namoi Catchment Irrigation Profile*.

Irish, R. R. (2000). *Landsat 7 automatic cloud cover assessment* (S. S. Shen & M. R. Descour, Eds.; p. 348). https://doi.org/10.1117/12.410358

Irish, R. R., Barker, J. L., Goward, S. N., & Arvidson, T. (2006). Characterization of the Landsat-7 ETM+ Automated Cloud-Cover Assessment (ACCA) Algorithm. *Photogrammetric Engineering & Remote Sensing*, *72*(10), 1179–1188. https://doi.org/10.14358/PERS.72.10.1179

Isbell, R. (2016). *The Australian soil classification* (3rd ed.). CSIRO Publishing.

Jensen, J. R. (2021). *Introductory Digital Image Processing: A Remote Sensing Perspective* (4th ed.). Pearson.

Ji, Z., Pan, Y., Zhu, X., Wang, J., & Li, Q. (2021). Prediction of Crop Yield Using Phenological Information Extracted from Remote Sensing Vegetation Index. *Sensors*, *21*(4), 1406. https://doi.org/10.3390/s21041406

Ju, J., & Roy, D. P. (2008). The availability of cloud-free Landsat ETM+ data over the conterminous United States and globally. *Remote Sensing of Environment*, *112*(3), 1196–1211. https://doi.org/10.1016/j.rse.2007.08.011

Katari, S., Bhowmik, T. K., Nair, S. S., Nayak, A. R., & Pankajakshan, P. (2022). Crop Phenology Stage Forecasting and Detection using NDVI Time-Series and LSTM. *IGARSS 2022 - 2022 IEEE International Geoscience and Remote Sensing Symposium*.

Knipling, E. B. (1970). Physical and physiological basis for the reflectance of visible and near-infrared radiation from vegetation. *Remote Sensing of Environment*, *1*(3).

Li, F., Jupp, D. L. B., Reddy, S., Lymburner, L., Mueller, N., Tan, P., & Islam, A. (2010). An Evaluation of the Use of Atmospheric and BRDF Correction to Standardize Landsat Data. *IEEE Journal of Selected Topics in Applied Earth Observations and Remote Sensing*, *3*(3), 257–270. https://doi.org/10.1109/JSTARS.2010.2042281

Li, F., Jupp, D. L. B., Thankappan, M., Lymburner, L., Mueller, N., Lewis, A., & Held, A. (2012). A physics-based atmospheric and BRDF correction for Landsat data over mountainous terrain. *Remote Sensing of Environment*, *124*, 756–770. https://doi.org/10.1016/j.rse.2012.06.018

Liu, J., Pattey, E., & Jégo, G. (2012). Assessment of vegetation indices for regional crop green LAI estimation from Landsat images over multiple growing seasons. *Remote Sensing of Environment*, *123*, 347–358. https://doi.org/10.1016/j.rse.2012.04.002

Mas, J.-F. (1999). Monitoring land-cover changes: A comparison of change detection techniques. *International Journal of Remote Sensing*, *20*(1), 139–152. https://doi.org/10.1080/014311699213659

Mayaux, P., Bartholomé, E., Fritz, S., & Belward, A. (2004). A new land-cover map of Africa for the year 2000. *Journal of Biogeography*, *31*(6), 861–877. https://doi.org/10.1111/j.1365-2699.2004.01073.x

Nguy-Robertson, A., Gitelson, A., Peng, Y., Viña, A., Arkebauer, T., & Rundquist, D. (2012). Green Leaf Area Index Estimation in Maize and Soybean: Combining Vegetation Indices to Achieve Maximal Sensitivity. *Agronomy Journal*, *104*(5), 1336–1347. https://doi.org/10.2134/agronj2012.0065

Pan, Z., Huang, J., Zhou, Q., Wang, L., Cheng, Y., Zhang, H., Blackburn, G. A., Yan, J., & Liu, J. (2015). Mapping crop phenology using NDVI time-series derived from HJ-1 A/B data. *International Journal of Applied Earth Observation and Geoinformation*, *34*, 188–197. https://doi.org/10.1016/j.jag.2014.08.011

Paruelo, J. M., Jobbágy, E. G., & Sala, O. E. (2001). Current Distribution of Ecosystem Functional Types in Temperate South America. *Ecosystems*, *4*(7), 683–698. https://doi.org/10.1007/s10021-001-0037-9

Pervez, M. S., & Brown, J. F. (2010). Mapping Irrigated Lands at 250-m Scale by Merging MODIS Data and National Agricultural Statistics. *Remote Sensing*, *2*(10), 2388–2412. https://doi.org/10.3390/rs2102388

Pu, R., Gong, P., Tian, Y., Miao, X., Carruthers, R. I., & Anderson, G. L. (2008). Using classification and NDVI differencing methods for monitoring sparse vegetation coverage: a case study of saltcedar in Nevada, USA. *International Journal of Remote Sensing*, *29*(14), 3987–4011. https://doi.org/10.1080/01431160801908095

Qiu, S., Zhu, Z., & Woodcock, C. E. (2020). Cirrus clouds that adversely affect Landsat 8 images: What are they and how to detect them? *Remote Sensing of Environment*, *246*, 111884. https://doi.org/10.1016/j.rse.2020.111884

Ridd, M. K., & Liu, J. (1998). A Comparison of Four Algorithms for Change Detection in an Urban Environment. *Remote Sensing of Environment*, *63*(2), 95–100. https://doi.org/10.1016/S0034-4257(97)00112-0

Rodriguez, D., deVoil, P., Power, B., Cox, H., Crimp, S., & Meinke, H. (2011). The intrinsic plasticity of farm businesses and their resilience to change. An Australian example. *Field Crops Research*, *124*(2), 157–170. https://doi.org/10.1016/j.fcr.2011.02.012

Rouse, J. W. , Jr., Haas, R. H., Schell, J. A., & Deering, D. W. (1974). Monitoring vegetation systems in the Great Plains with ERTS. In S. C. Freden, E. P. Mercanti, & M. A. Becker (Eds.), *Third Earth Resources Technology Satellite-1 Symposium- Volume I: Technical Presentations* (p. 309). NASA.

Sacks, W. J., Deryng, D., Foley, J. A., & Ramankutty, N. (2010). Crop planting dates: an analysis of global patterns. *Global Ecology and Biogeography*, no-no. https://doi.org/10.1111/j.1466-8238.2010.00551.x

Shahriar Pervez, Md., Budde, M., & Rowland, J. (2014). Mapping irrigated areas in Afghanistan over the past decade using MODIS NDVI. *Remote Sensing of Environment*, *149*, 155–165. https://doi.org/10.1016/j.rse.2014.04.008

Shanahan, J. F., Holland, K. H., Schepers, J. S., Francis, D. D., Schlemmer, M. R., & Caldwell, R. (2015). *Use of a Crop Canopy Reflectance Sensor to Assess Corn Leaf Chlorophyll Content* (pp. 135–150). https://doi.org/10.2134/asaspecpub66.c11

Singh, A. (1989). Review Article Digital change detection techniques using remotely-sensed data. *International Journal of Remote Sensing*, *10*(6), 989–1003. https://doi.org/10.1080/01431168908903939

Tennakoon, S. B., & Milroy, S. P. (2003). Crop water use and water use efficiency on irrigated cotton farms in Australia. *Agricultural Water Management*, *61*(3), 179–194. https://doi.org/10.1016/S0378-3774(03)00023-4

Thomas, M. (2001). *Remote sensing in South Australia's land condition monitoring project*.

Tilling, A. K., O'Leary, G. J., Ferwerda, J. G., Jones, S. D., Fitzgerald, G. J., Rodriguez, D., & Belford, R. (2007). Remote sensing of nitrogen and water stress in wheat. *Field Crops Research*, *104*(1–3), 77–85. https://doi.org/10.1016/j.fcr.2007.03.023

Tucker, C. J., & Choudhury, B. J. (1987). Satellite remote sensing of drought conditions. *Remote Sensing of Environment*, *23*(2), 243–251. https://doi.org/10.1016/0034-4257(87)90040-X

Wang, J., Rich, P. M., & Price, K. P. (2003). Temporal responses of NDVI to precipitation and temperature in the central Great Plains, USA. *International Journal of Remote Sensing*, *24*(11), 2345–2364. https://doi.org/10.1080/01431160210154812

Wardlow, B. D., & Egbert, S. L. (2008). Large-area crop mapping using time-series MODIS 250 m NDVI data: An assessment for the U.S. Central Great Plains. *Remote Sensing of Environment*, *112*(3), 1096–1116. https://doi.org/10.1016/j.rse.2007.07.019

Welsh, W., Hodgkinson, J., Strand, J., Northey, J., Aryal, S., O'Grady, A., Slatter, E., Herron, N., Pinetown, K., Carey, H., Yates, G., Raisbeck-Brown, N., & Lewis, S. (2014). *Context statement for the Namoi subregion. Product 1.1 from the Northern Inland Catchments Bioregional Assessment*.

Wilson, T. B., & Meyers, T. P. (2007). Determining vegetation indices from solar and photosynthetically active radiation fluxes. *Agricultural and Forest Meteorology*, *144*(3–4), 160–179. https://doi.org/10.1016/j.agrformet.2007.04.001

Yang, Y., Tao, B., Liang, L., Huang, Y., Matocha, C., Lee, C. D., Sama, M., Masri, B. El, & Ren, W. (2021). Detecting Recent Crop Phenology Dynamics in Corn and Soybean Cropping Systems of Kentucky. *Remote Sensing*, *13*(9), 1615. https://doi.org/10.3390/rs13091615

You, X., Meng, J., Zhang, M., & Dong, T. (2013). Remote Sensing Based Detection of Crop Phenology for Agricultural Zones in China Using a New Threshold Method. *Remote Sensing*, *5*(7), 3190–3211. https://doi.org/10.3390/rs5073190

Zhu, Z., Wang, S., & Woodcock, C. E. (2015). Improvement and expansion of the Fmask algorithm: cloud, cloud shadow, and snow detection for Landsats 4–7, 8, and Sentinel 2 images. *Remote Sensing of Environment*, *159*, 269–277. https://doi.org/10.1016/j.rse.2014.12.014